Available online at www.sciencedirect.com
SCIENCE DIRECT®
Annals of Nuclear Energy 31 (2004) 1555–1582
annals of NUCLEAR ENERGY
www.elsevier.com/locate/anucene

A finite element/boundary element hybrid method for 2-D neutron diffusion calculations

S. Cavdar, H.A. Ozgener *

Institute of Energy, Istanbul Technical University, Maslak, Istanbul 80626, Turkey

Received 8 March 2004; accepted 21 April 2004
Available online 11 June 2004

Abstract

A finite element-boundary element hybrid method has been developed for one or two group neutron diffusion calculations. A linear or bilinear finite element formulation for the reactor core and a linear boundary element technique for the reflector which are combined through interface continuity conditions constitute the basis of the developed method. The present formulation is restricted to two-dimensional geometries and has been implemented in the developed computer program. Via comparisons with analytical solutions, the proposed method has been validated. Further comparisons against the pure finite and boundary element formulations show that the proposed method constitutes a viable alternative for the numerical solution of neutron diffusion problems of both the external neutron source and multiplication eigenvalue determination variety.

1. Introduction

The finite element method (FEM) is a well-established method in applied mathematics and engineering. It is preferred in most applications to its principal alternative, the finite difference method (FDM), due to its flexibility in the treatment of curved or irregular geometries and the high rates of convergence attainable by the use of high order elements. The first prototype engineering application of FEM was

* Corresponding author. Tel.: +90-212-285-3943; fax: +90-212-285-3884.
E-mail address: ozgenera@itu.edu.tr (H.A. Ozgener).

0306-4549/$ - see front matter © 2004 Elsevier Ltd. All rights reserved.
doi:10.1016/j.anucene.2004.04.006

in the field structural engineering and dates back to 1956 (Turner et al., 1956). A very early variational finite element type solution procedure using the principle of minimum potential energy and linear triangular elements was seen in the field of applied mathematics (Courant, 1943). Starting from 1960s the applied mathematics and engineering streams of development have started to converge and FEM became a most extensively used technique in almost every branch of engineering and mathematical physics. The first application of FEM to the theory of neutron diffusion dates back to 1970s. The developments in the application FEM to the neutron diffusion and even-parity transport equations have been described in the excellent treatise of Lewis (1981).

The boundary element method (BEM) is a newer method compared to FEM. It is based upon the conversion of the governing differential equation into a boundary integral equation (BIE) via Green's second identity and infinite medium Green's functions (fundamental solutions). Since the resulting BIE involves unknowns only on the system boundary, the dimension of the problem is almost reduced by one. Although it is possible to trace back a formal presentation of the basic ideas of BEM to the works of the Russian author Mikhlin (1965), it is generally accepted (Brebbia et al., 1984), that at least "direct" BEM originated in the work of Cruse and Rizzo (1968). The expansion of the use of BEM to different fields of engineering and mathematical physics has been especially faster after the use of the term "Boundary Element" in a textbook (Brebbia, 1978). The first application of BEM to the neutron diffusion equation dates back to middle 1980s (Itagaki, 1985). Further research in the application of BEM to the neutron diffusion equation concentrated on preserving the "boundary only" philosophy of BEM by converting the scattering volume integrals (Ozgener, 1998) and external neutron source volume integrals (Ozgener and Ozgener, 1994) into surface integrals.

Recent investigations in the application of BEM to the neutron diffusion equation concentrated on the solution of multi-region problems. In BEM formulations developed for the solution of multiregion problems, two distinct approaches have been taken. In the approach which might be referred as the classical BEM approach, the BEM equations for each of the homogeneous regions in the system are assembled together in a block matrix form using the concept of the "virtual side" and the continuity of the flux and current across material interfaces (Ozgener and Ozgener, 2001). Although group-to-group scattering domain integrals are reduced to boundary integrals via a recently developed BIE (Ozgener, 1998), fission source domain integrals have still to be evaluated and the determination of the effective multiplication factor (k_{eff}) proceeds through the classical fission source iteration procedure of nuclear reactor analysis. The second approach which might be referred as the domain decomposition BEM proceeds without utilizing the fission source iteration procedure and is based on the domain decomposition method. The most important advantage of this approach is the elimination of both group-to-group scattering and fission source domain integrals. Domain decomposition BEM is based on the diagonalization of the k-estimate dependent infinite medium matrix of each homogeneous region, by a similarity transformation. By this process, the multiregion diffusion equations for each homogeneous region is

transformed into a set of homogenous or nonhomogeneous (if there is an external source) equations which are either of the Helmholtz or modified Helmholtz type, depending on the sign of the eigenvalues of the infinite medium matrix. There are two variants of the domain decomposition BEM. In the first variant which is called the hierarchical domain decomposition boundary element method (HDD-BEM) (Purwadi et al., 1998), a two-level calculation procedure is employed. At the lower level, the Helmholtz (or modified Helmholtz) type mode equations are solved by constant BEM for each homogeneous region using estimates of the multiplication factor and nodal values of the mode functions. At the higher level, the multiplication factor and nodal values of the mode functions assumed at interfaces are modified by Newton's method to satisfy the continuity conditions for the neutron flux and current at interfaces. The computational performance of the original HDD-BEM has been enhanced by using higher-order boundary elements instead of constant ones in 2-D calculations (Chiba et al., 2001a). The optimization of the computational performance of the HDD-BEM has also been one of the main concerns of this work. The HDD-BEM has recently been extended to 3-D-problems (Chiba et al., 2001b). The second variant of the domain decomposition BEM is called the response matrix boundary element method (RM-BEM) (Maiani and Montagnini, 1999). RM-BEM depends also on domain decomposition and employs a two-level hierarchical procedure like HDD-BEM. In RM-BEM, the BIE's of each homogeneous region are expressed in terms of inward and outward partial current currents at the region boundaries. The response matrix (RM) of each region relates the outward partial current to the inward partial current. The partial currents are determined using an iterative method.

FEM and BEM have both advantages and disadvantages relative to each other. Since BEM restricts the unknowns to region boundaries, the linear system dimensions resulting from BEM discretization are greatly reduced relative to FEM discretization. But the full and nonsymmetric nature of the coefficient matrix of BEM is clearly a disadvantage relative to the symmetric, sparse and positive-definite FEM coefficient matrix. Since the emergence of FEM and BEM as numerical solution techniques, many researchers in different areas of engineering and mathematical physics tried to combine FEM and BEM in the solution of their problems in order to exploit the advantages of both methods. Such FE/BE combined methods are usually termed as hybrid methods. The first hybrid FE/BE formulation was first suggested by Zienkiewicz et al. (1977). Since that time, many variants of FE/BE hybrid formulations have been proposed in various branches of engineering (Brebbia and Georgios, 1979). Many recent research efforts Guven and Madenci (2003), Pascal et al. (2003) and Gail et al. (2002) involve hybrid FE/BE formulations which take specific physical characteristics of the analyzed systems into account. Although both FEM and BEM have been separately applied in the field of neutron diffusion, a hybrid FE/BE formulation has not been suggested. In this paper, we'll propose a hybrid FE/BE formulation for two region reflected systems using the classical approach without resorting to domain decomposition procedures. Such a hybrid FE/BE method, using a FEM formulation in the core and a BEM formulation in the reflector seems attractive for two reasons. For one

thing, FEM has proved itself to be a very efficient discretization method especially in regions where neutron sources are present like a reactor core. For another, BEM is very efficient especially in regions like reflectors where no fission neutron sources are present. No internal mesh is necessary even if domain decomposition methods are not employed. The FE/BE hybrid formulation we'll develop in this paper is directed towards nuclear systems consisting of the core and reflector regions. The development will be within the context of group diffusion theory restricted to one or two groups. The validation of the developed method will be carried out by comparison with analytical solutions. Although the relative merit of the suggested method will be assessed via comparisons with pure BEM and FEM solutions, optimization of the computational performance of the suggested technique is not among our aims in this work.

2. Formulation

2.1. Governing equations

We consider a nuclear system consisting of a nuclear reactor core (C) and a reflector, (R). The volume and outer surface of the core and reflector are denoted by V^k and S^k where $k = C$ or R. The core-reflector interface (I) is denoted by S^{I}. We assume that the core and reflector outer surface may consist of two nonoverlapping parts; a part over which vacuum boundary conditions (v) prevail and another part over which reflection boundary condition (r) is prescribed. Thus $S^{\mathrm{C}} = S_v^{\mathrm{C}} \cup S_r^{\mathrm{C}}$ and $S^{\mathrm{R}} = S_v^{\mathrm{R}} \cup S_r^{\mathrm{R}}$. A picture of the described nuclear system is presented in Fig. 1. If we let the energy group index g be 1 or 2, corresponding to first and second energy groups, the two-group diffusion equations can be written generally as

$$-D_g^j \nabla^2 \Phi_g(\vec{r}) + \Sigma_{\mathrm{r},g}^j \Phi_g(\vec{r}) = s_g\left(\vec{r}\right), \quad \vec{r} \in V^j, \ \ j = C \text{ or } R, \tag{1}$$

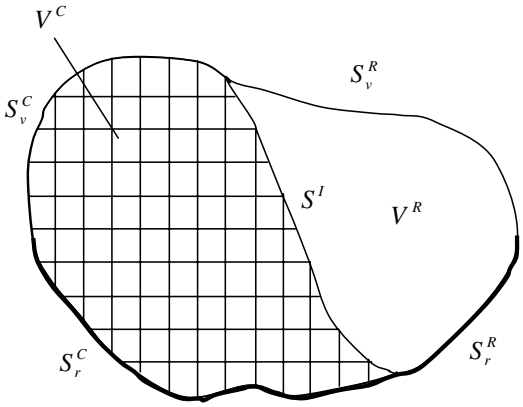

Fig. 1. Nuclear system consisting of the core and the reflector.

D_g^j, $\Sigma_{r,g}^j$ and $s_g^j(\vec{r})$ represent the group diffusion constant, the group removal cross section and group neutron source of the core ($j = C$) or the reflector ($j = R$). $\Phi_g(\vec{r})$ is the g'th group neutron flux. Before FEM or BEM discretization, (1) is usually cast into the form:

$$\nabla^2 \Phi_g(\vec{r}) - \left(k_g^j\right)^2 \Phi_g(\vec{r}) = -\frac{s_g(\vec{r})}{D_g^j}, \quad \vec{r} \in V^j, \ \ j = C \text{ or } R, \tag{2}$$

where the inverse diffusion length is defined as

$$k_g^j = \sqrt{\frac{\Sigma_{r,g}^j}{D_g^j}}. \tag{3}$$

Both the FEM formulation for the core and BEM formulation for the reflector is based on the definition of the residual function:

$$R_g^j(\vec{r}) = \nabla^2 \phi_g(\vec{r}) - \left(k_g^j\right)^2 \phi_g(\vec{r}) + \frac{s_g^j(\vec{r})}{D_g^j}, \quad \vec{r} \in V^j, \ \ j = C \text{ or } R, \tag{4}$$

where $\phi_g(\vec{r})$ is some approximation to $\Phi_g(\vec{r})$. The residual is identically equal to zero when $\phi_g(\vec{r}) = \Phi_g(\vec{r})$, the actual neutron flux. Both BEM and FEM are based on the requirement that at least the weighted integral of the residual function $R_g^j(\vec{r})$ over the system volume vanish for $\phi_g(\vec{r})$, some approximation to $\Phi_g(\vec{r})$, with some predetermined space of weight functions; $w(\vec{r})$:

$$\int_{V^j} w(\vec{r}) R_g^j(\vec{r}) \mathrm{d}V = 0, \quad g = 1, 2, \ \ j = C \text{ or } R. \tag{5}$$

Different choices for the weight function, $w(\vec{r})$ and the approximation to the neutron flux, $\phi_g(\vec{r})$, lead to different BEM and FEM formulations.

In the formulation for the core, (5) is in the form:

$$\int_{V^C} w(\vec{r}) \left[\nabla^2 \phi_g(\vec{r}) - \left(k_g^C\right)^2 \phi_g(\vec{r}) + \frac{s_g(\vec{r})}{D_g^C} \right] \mathrm{d}V = 0. \tag{6}$$

For arriving at the equation which forms the basis of FEM formulation, we apply Green's First Identity to the first term of (6) to obtain:

$$\int_{V^C} \left[\vec{\nabla} w(\vec{r}) \cdot \vec{\nabla} \phi_g(\vec{r}) + \left(k_g^C\right)^2 w(\vec{r}) \phi_g(\vec{r}) - w(\vec{r}) \frac{s_g(\vec{r})}{D_g^C} \right] \mathrm{d}V - \int_{\tilde{S}^C} w(\vec{r}) \frac{\partial \phi_g}{\partial n}(\vec{r}) \mathrm{d}S = 0, \tag{7}$$

where $\tilde{S}^j = S^j \cup S^I, j = C$ or R and n is the outward normal direction at any point on $\tilde{S}^j$. If we express the normal derivative in terms of the component of the group g neutron current $\vec{J}_g(\vec{r})$ as

$$J_g(\vec{r}) = -D_g^j \frac{\partial \phi_g}{\partial n}(\vec{r}), \quad \vec{r} \in \tilde{S}^j \tag{8}$$

and apply the reflection boundary condition:

$$J_g(\vec{r}) = 0, \quad \vec{r} \in S_r^j, \ \ j = C \text{ or } R \tag{9}$$

and the vacuum boundary condition:

$$\tfrac{1}{4}\phi_g(\vec{r}) - \tfrac{1}{2}J_g(\vec{r}) = 0, \quad \vec{r} \in S_v^j, \ \ j = C \text{ or } R, \tag{10}$$

(7) becomes:

$$\int_{V^C} \left[\vec{\nabla} w(\vec{r}) \cdot \vec{\nabla} \phi_g(\vec{r}) + \left(k_g^C\right)^2 w(\vec{r}) \phi_g(\vec{r}) - w(\vec{r}) \frac{s_g(\vec{r})}{D_g^C} \right] \mathrm{d}V + \frac{1}{2D_g^C} \times \int_{S_v^C} w(\vec{r}) \phi_g(\vec{r}) \mathrm{d}S + \frac{1}{D_g^C} \int_{S^I} w(\vec{r}) J_g(\vec{r}) \mathrm{d}S = 0, \tag{11}$$

(11) constitutes the starting point for the FEM discretization of the reactor core.

In the formulation for the reflector, (5) is in the form:

$$\int_{V^R} w(\vec{r}) \left[\nabla^2 \phi_g(\vec{r}) - \left(k_g^R\right)^2 \phi_g(\vec{r}) + \frac{s_g(\vec{r})}{D_g^R} \right] \mathrm{d}V = 0. \tag{12}$$

For arriving at the equation which forms the basis of the BEM formulation, we apply Green's Second Identity to the first term of (12) to obtain:

$$\int_{V^R} \phi_g(\vec{r}) \left[\nabla^2 w(\vec{r}) - \left(k_g^R\right)^2 w(\vec{r}) + \frac{w(\vec{r}) s_g(\vec{r})}{D_g^R} \right] \mathrm{d}V + \int_{\tilde{S}^R} w(\vec{r}) \frac{\partial \phi_g}{\partial n}(\vec{r}) \mathrm{d}S - \int_{\tilde{S}^R} \phi_g(\vec{r}) \frac{\partial w}{\partial n}(\vec{r}) \mathrm{d}S = 0. \tag{13}$$

Applying (8)–(10); (13) is cast into the form:

$$\int_{V^R} \phi_g(\vec{r}) \left[\nabla^2 w(\vec{r}) - \left(k_g^R\right)^2 w(\vec{r}) + \frac{w(\vec{r}) s_g(\vec{r})}{D_g^R} \right] \mathrm{d}V - \int_{S^I} \left[\frac{w(\vec{r})}{D_g^R} J_g(\vec{r}) + \phi_g(\vec{r}) \frac{\partial w}{\partial n}(\vec{r}) \right] \mathrm{d}S - \int_{S_v^R} \phi_g(\vec{r}) \left[\frac{w(\vec{r})}{2D_g^R} + \frac{\partial w}{\partial n}(\vec{r}) \right] \mathrm{d}S - \int_{S_r^R} \phi_g(\vec{r}) \frac{\partial w}{\partial n}(\vec{r}) \mathrm{d}S = 0. \tag{14}$$

Eq. (14) constitutes the starting point for the BEM discretization of the reflector.

2.2. FEM discretization of the reactor core

For the FEM discretization of the reactor core, we assume a 2-D model and introduce a mesh of linear triangular or bilinear quadrilateral mesh of finite elements over the reactor core as shown in Fig. 2. The nodes which are not on the core-reflector interface are called non-interface nodes and are numbered from $j = 1$ to N_C.

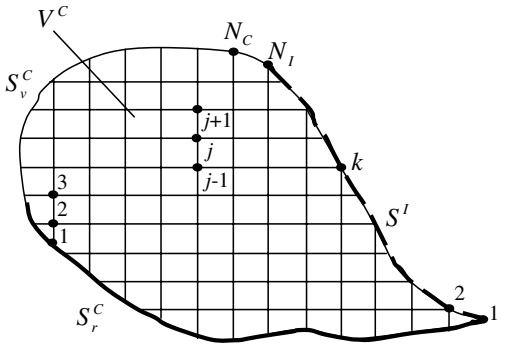

Fig. 2. Finite element mesh for the core.

On the other hand, the nodes on the core-reflector interface are numbered separately from $k = 1$ to N_{I}. The piecewise linear or bilinear finite element trial function belonging to non-interface nodes j and interface nodes k are denoted by $h_j^{\mathrm{C}}(\vec{r})(j = 1,\ldots,N_{\mathrm{C}})$ and $h_k^{\mathrm{I}}(\vec{r})(k = 1,\ldots,N_{\mathrm{I}})$ respectively. We express both the weight function, $w(\vec{r})$, and the approximation to the group flux, $\phi_g(\vec{r})$ in (11) in terms of the finite element trial functions as

$$w(\vec{r}) = \left(\underline{w}^{\mathrm{C}}\right)^{\mathrm{T}}\underline{h}^{\mathrm{C}}(\vec{r}) + \left(\underline{w}^{\mathrm{I}}\right)^{\mathrm{T}}\underline{h}^{\mathrm{I}}(\vec{r}), \tag{15}$$

$$\phi_g(\vec{r}) = \left(\underline{\phi}_g^{\mathrm{C}}\right)^{\mathrm{T}}\underline{h}^{\mathrm{C}}(\vec{r}) + \left(\underline{\phi}_g^{\mathrm{I}}\right)^{\mathrm{T}}\underline{h}^{\mathrm{I}}(\vec{r}), \tag{16}$$

where the N_{C} dimensional vectors $\underline{w}^{\mathrm{C}}, \underline{\phi}_g^{\mathrm{C}}$ and N_{I} dimensional vectors $\underline{w}^{\mathrm{I}}, \underline{\phi}_g^{\mathrm{I}}$ contain the function values at the nodes as their elements. We also assume a linear variation of current over the core-reflector interface and write:

$$J_g(\vec{r}) = \left(\underline{J}_g^{\mathrm{I}}\right)^{\mathrm{T}}\underline{h}^{\mathrm{I}}(\vec{r}), \quad \vec{r} \in S^{\mathrm{I}}. \tag{17}$$

When we substitute (15)–(17) into (11), we obtain:

$$\left(\underline{w}^{\mathrm{C}}\right)^{\mathrm{T}}\left[\underline{\underline{A}}_g^{\mathrm{C}}\underline{\phi}_g^{\mathrm{C}} + \underline{\underline{A}}_g^{\mathrm{CI}}\underline{\phi}_g^{\mathrm{I}} - \underline{q}_g^{\mathrm{C}}\right] + \left(\underline{w}^{\mathrm{I}}\right)^{\mathrm{T}}\left[\underline{\underline{A}}_g^{\mathrm{I}}\underline{\phi}_g^{\mathrm{I}} + \underline{\underline{A}}_g^{\mathrm{IJ}}\underline{J}_g^{\mathrm{I}} + \left(\underline{\underline{A}}_g^{\mathrm{CI}}\right)^{\mathrm{T}}\underline{\phi}_g^{\mathrm{C}} - \underline{q}_g^{\mathrm{I}}\right] = 0. \tag{18}$$

The $N_{\mathrm{C}} \times N_{\mathrm{C}}$ square matrix $\underline{\underline{A}}_g^{\mathrm{C}}$, $N_{\mathrm{C}} \times N_{\mathrm{I}}$ rectangular matrix $\underline{\underline{A}}_g^{\mathrm{CI}}$, and the two $N_{\mathrm{I}} \times N_{\mathrm{I}}$ square matrices $\underline{\underline{A}}_g^{\mathrm{I}}$ and $\underline{\underline{A}}_g^{\mathrm{IJ}}$ are defined below:

$$\underline{\underline{A}}_g^{\mathrm{C}} = \int_{V^{\mathrm{C}}} \left\{ \vec{\nabla}\underline{h}^{\mathrm{C}}(\vec{r}) \cdot \vec{\nabla}\left[\underline{h}^{\mathrm{C}}(\vec{r})\right]^{\mathrm{T}} + \left(k_g^{\mathrm{C}}\right)^2 \underline{h}^{\mathrm{C}}(\vec{r})\left[\underline{h}^{\mathrm{C}}(\vec{r})\right]^{\mathrm{T}} \right\} \mathrm{d}V + \frac{1}{2D_g^{\mathrm{C}}} \times \int_{S_v^{\mathrm{C}}} \underline{h}^{\mathrm{C}}(\vec{r})\left[\underline{h}^{\mathrm{C}}(\vec{r})\right]^{\mathrm{T}} \mathrm{d}S, \tag{19}$$

$$\underline{\underline{A}}_g^{\mathrm{CI}} = \int_{V^{\mathrm{C}}} \left\{ \vec{\nabla}\underline{h}^{\mathrm{C}}(\vec{r}) \cdot \vec{\nabla}\left[\underline{h}^{\mathrm{I}}(\vec{r})\right]^{\mathrm{T}} + \left(k_g^{\mathrm{C}}\right)^2 \underline{h}^{\mathrm{C}}(\vec{r})\left[\underline{h}^{\mathrm{I}}(\vec{r})\right]^{\mathrm{T}} \right\} \mathrm{d}V + \frac{1}{2D_g^{\mathrm{C}}} \times \int_{S_v^{\mathrm{C}}} \underline{h}^{\mathrm{C}}(\vec{r})\left[\underline{h}^{\mathrm{I}}(\vec{r})\right]^{\mathrm{T}} \mathrm{d}S, \tag{20}$$

$$\underline{\underline{A}}_g^{\mathrm{I}} = \int_{V^{\mathrm{C}}} \left\{ \vec{\nabla}\underline{h}^{\mathrm{I}}(\vec{r}) \cdot \vec{\nabla}\left[\underline{h}^{\mathrm{I}}(\vec{r})\right]^{\mathrm{T}} + \left(k_g^{\mathrm{C}}\right)^2 \underline{h}^{\mathrm{I}}(\vec{r})\left[\underline{h}^{\mathrm{I}}(\vec{r})\right]^{\mathrm{T}} \right\} \mathrm{d}V, \tag{21}$$

$$\underline{\underline{A}}_g^{\mathrm{IJ}} = \frac{1}{D_g^{\mathrm{C}}} \int_{V^{\mathrm{C}}} \underline{h}^{\mathrm{I}}(\vec{r})\left[\underline{h}^{\mathrm{I}}(\vec{r})\right]^{\mathrm{T}} \mathrm{d}V. \tag{22}$$

The N_{C} dimensional vector $\underline{q}_g^{\mathrm{C}}$ and N_{I} dimensional vector $\underline{q}_g^{\mathrm{I}}$ are defined as

$$\underline{q}_g^{\mathrm{C}} = \frac{1}{D_g^{\mathrm{C}}} \int_{V^{\mathrm{C}}} s_g(\vec{r})\underline{h}^{\mathrm{C}}(\vec{r})\mathrm{d}V, \tag{23}$$

$$\underline{q}_g^{\mathrm{I}} = \frac{1}{D_g^{\mathrm{C}}} \int_{V^{\mathrm{C}}} s_g(\vec{r})\underline{h}^{\mathrm{I}}(\vec{r})\mathrm{d}V. \tag{24}$$

For (18) to vanish for arbitrary $\underline{w}^{\mathrm{C}}$ and $\underline{w}^{\mathrm{I}}$ we must have:

$$\underline{\underline{A}}_g^{\mathrm{C}}\underline{\phi}_g^{\mathrm{C}} + \underline{\underline{A}}_g^{\mathrm{CI}}\underline{\phi}_g^{\mathrm{I}} = \underline{q}_g^{\mathrm{C}}, \tag{25}$$

$$\left(\underline{\underline{A}}_g^{\mathrm{CI}}\right)^{\mathrm{T}}\underline{\phi}_g^{\mathrm{C}} + \underline{\underline{A}}_g^{\mathrm{I}}\underline{\phi}_g^{\mathrm{I}} + \underline{\underline{A}}_g^{\mathrm{IJ}}\underline{J}_g^{\mathrm{I}} = \underline{q}_g^{\mathrm{I}}. \tag{26}$$

The matrices $\underline{\underline{A}}_g^{\mathrm{C}}$ and $\underline{\underline{A}}_g^{\mathrm{I}}$ are symmetric and sparse due to the compact support of finite element trial functions.

The group source $s_g(\vec{r})$ consists of the fission/external source and the scattering source for $g = 2$. If we are using two-group theory, we can write:

$$s_g(\vec{r}) = \frac{\chi_g}{k}\sum_{g'=1}^{2} \upsilon\Sigma_{\mathrm{f},g'}^{\mathrm{C}}\phi_{g'}(\vec{r}) + Q_g(\vec{r}) + \delta_{g,2}\Sigma_{\mathrm{s},2\leftarrow 1}^{\mathrm{C}}\phi_1(\vec{r}), \tag{27}$$

where χ_g and $\upsilon\Sigma_{\mathrm{f},g}^{\mathrm{C}}$ represent the group fission spectrum fraction and the fission yield cross section of the core respectively. k is the latest estimate for the system effective multiplication factor (k_{eff}) during fission source iteration. $Q_g(\vec{r})$ is the group external neutron source. $\Sigma_{\mathrm{s},2\leftarrow 1}^{\mathrm{C}}$ is the scattering cross section from group 1 to group 2 of the core. Since we solve either fission source iteration or external source problems, either the first or the second term on the right hand side of (27) is present, but not both. If we use the FEM expansion (16) in (27) and then insert the resulting expression into (23) and (24) (thus employ the "consistent source approximation" (Ozgener, 1990)), we obtain:

$$\underline{q}_g^{\mathrm{C}} = \frac{1}{k}\sum_{g'=1}^{2}\left[\underline{\underline{F}}_{g\leftarrow g'}^{\mathrm{C}}\underline{\phi}_{g'}^{\mathrm{C}} + \underline{\underline{F}}_{g\leftarrow g'}^{\mathrm{CI}}\underline{\phi}_{g'}^{\mathrm{I}}\right] + \underline{S}_g^{\mathrm{C}} + \delta_{g,2}\left[\underline{\underline{S}}_{2\leftarrow 1}^{\mathrm{C}}\underline{\phi}_1^{\mathrm{C}} + \underline{\underline{S}}_{2\leftarrow 1}^{\mathrm{CI}}\underline{\phi}_1^{\mathrm{I}}\right], \tag{28}$$

$$\underline{q}_g^{\mathrm{I}} = \frac{1}{k}\sum_{g'=1}^{2}\left[\left(\underline{\underline{F}}_{g\leftarrow g'}^{\mathrm{CI}}\right)^{\mathrm{T}}\underline{\phi}_{g'}^{\mathrm{C}} + \underline{\underline{F}}_{g\leftarrow g'}^{\mathrm{I}}\underline{\phi}_{g'}^{\mathrm{I}}\right] + \underline{S}_g^{\mathrm{I}} + \delta_{g,2}\left[\left(\underline{\underline{S}}_{2\leftarrow 1}^{\mathrm{CI}}\right)^{\mathrm{T}}\underline{\phi}_1^{\mathrm{C}} + \underline{\underline{S}}_{2\leftarrow 1}^{\mathrm{I}}\underline{\phi}_1^{\mathrm{I}}\right], \quad (29)$$

where the $N_{\mathrm{C}} \times N_{\mathrm{C}}$ square matrices:

$$\underline{\underline{F}}_{g\leftarrow g'}^{\mathrm{C}} = \frac{\chi_g \upsilon \Sigma_{\mathrm{f},g'}^{\mathrm{C}}}{D_g^{\mathrm{C}}}\int_{V^{\mathrm{C}}} \underline{h}^{\mathrm{C}}(\vec{r})\left[\underline{h}^{\mathrm{C}}(\vec{r})\right]^{\mathrm{T}}\mathrm{d}V, \quad (30)$$

$$\underline{\underline{S}}_{2\leftarrow 1}^{\mathrm{C}} = \frac{\Sigma_{\mathrm{s},2\leftarrow 1}^{\mathrm{C}}}{D_1^{\mathrm{C}}}\int_{V^{\mathrm{C}}} \underline{h}^{\mathrm{C}}(\vec{r})\left[\underline{h}^{\mathrm{C}}(\vec{r})\right]^{\mathrm{T}}\mathrm{d}V \quad (31)$$

are defined as above and have the same structure as $\underline{\underline{A}}_g^{\mathrm{C}}$. The $N_{\mathrm{C}} \times N_{\mathrm{I}}$ rectangular matrices which have the same structure as $\underline{\underline{A}}_g^{\mathrm{CI}}$ are:

$$\underline{\underline{F}}_{g\leftarrow g'}^{\mathrm{CI}} = \frac{\chi_g \upsilon \Sigma_{\mathrm{f},g'}^{\mathrm{C}}}{D_g^{\mathrm{C}}}\int_{V^{\mathrm{C}}} \underline{h}^{\mathrm{C}}(\vec{r})\left[\underline{h}^{\mathrm{I}}(\vec{r})\right]^{\mathrm{T}}\mathrm{d}V, \quad (32)$$

$$\underline{\underline{S}}_{2\leftarrow 1}^{\mathrm{CI}} = \frac{\Sigma_{\mathrm{s},2\leftarrow 1}^{\mathrm{C}}}{D_1^{\mathrm{C}}}\int_{V^{\mathrm{C}}} \underline{h}^{\mathrm{C}}(\vec{r})\left[\underline{h}^{\mathrm{I}}(\vec{r})\right]^{\mathrm{T}}\mathrm{d}V. \quad (33)$$

We have also the $N_{\mathrm{I}} \times N_{\mathrm{I}}$ square matrices:

$$\underline{\underline{F}}_{g\leftarrow g'}^{\mathrm{I}} = \frac{\chi_g \upsilon \Sigma_{\mathrm{f},g'}^{\mathrm{C}}}{D_g^{\mathrm{C}}}\int_{V^{\mathrm{C}}} \underline{h}^{\mathrm{I}}(\vec{r})\left[\underline{h}^{\mathrm{I}}(\vec{r})\right]^{\mathrm{T}}\mathrm{d}V, \quad (34)$$

$$\underline{\underline{S}}_{2\leftarrow 1}^{\mathrm{I}} = \frac{\Sigma_{\mathrm{s},2\leftarrow 1}^{\mathrm{C}}}{D_1^{\mathrm{C}}}\int_{V^{\mathrm{C}}} \underline{h}^{\mathrm{I}}(\vec{r})\left[\underline{h}^{\mathrm{I}}(\vec{r})\right]^{\mathrm{T}}\mathrm{d}V, \quad (35)$$

which have the same structure as $\underline{\underline{A}}_g^{\mathrm{I}}$. The N_{C} and N_{I} dimensional external source vectors are defined as

$$\underline{S}_g^{\mathrm{C}} = \frac{1}{D_g^{\mathrm{C}}}\int_{V^{\mathrm{C}}} Q_g(\vec{r})\underline{h}^{\mathrm{C}}(\vec{r})\mathrm{d}V, \quad (36)$$

$$\underline{S}_g^{\mathrm{I}} = \frac{1}{D_g^{\mathrm{C}}}\int_{V^{\mathrm{C}}} Q_g(\vec{r})\underline{h}^{\mathrm{I}}(\vec{r})\mathrm{d}V. \quad (37)$$

Finally, our FEM discretization of the core ends up with the following matricial equations which are obtained by combining (25), (26), (28) and (29) in the block matrix form:

$$\begin{bmatrix} \underline{\underline{A}}_g^{\mathrm{C}} & \underline{\underline{A}}_g^{\mathrm{CI}} & \underline{\underline{0}} \\ \left(\underline{\underline{A}}_g^{\mathrm{CI}}\right)^{\mathrm{T}} & \underline{\underline{A}}_g^{\mathrm{I}} & \underline{\underline{A}}_g^{\mathrm{IJ}} \end{bmatrix}\begin{bmatrix} \underline{\phi}_g^{\mathrm{C}} \\ \underline{\phi}_g^{\mathrm{I}} \\ \underline{J}_g^{\mathrm{I}} \end{bmatrix} = \frac{1}{k}\sum_{g'=1}^{2}\left\{\begin{bmatrix} \underline{\underline{F}}_{g\leftarrow g'}^{\mathrm{C}} & \underline{\underline{F}}_{g\leftarrow g'}^{\mathrm{CI}} & \underline{\underline{0}} \\ \left(\underline{\underline{F}}_{g\leftarrow g'}^{\mathrm{CI}}\right)^{\mathrm{T}} & \underline{\underline{F}}_{g\leftarrow g'}^{\mathrm{I}} & \underline{\underline{0}} \end{bmatrix}\begin{bmatrix} \underline{\phi}_{g'}^{\mathrm{C}} \\ \underline{\phi}_{g'}^{\mathrm{I}} \\ \underline{J}_{g'}^{\mathrm{I}} \end{bmatrix}\right\} + \begin{bmatrix} \underline{S}_g^{\mathrm{C}} \\ \underline{S}_g^{\mathrm{I}} \end{bmatrix} + \delta_{g,2}\begin{bmatrix} \underline{\underline{S}}_{2\leftarrow 1}^{\mathrm{C}} & \underline{\underline{S}}_{2\leftarrow 1}^{\mathrm{CI}} & \underline{\underline{0}} \\ \left(\underline{\underline{S}}_{2\leftarrow 1}^{\mathrm{CI}}\right)^{\mathrm{T}} & \underline{\underline{S}}_{2\leftarrow 1}^{\mathrm{I}} & \underline{\underline{0}} \end{bmatrix}\begin{bmatrix} \underline{\phi}_1^{\mathrm{C}} \\ \underline{\phi}_1^{\mathrm{I}} \\ \underline{J}_1^{\mathrm{I}} \end{bmatrix}. \quad (38)$$

In case of external source problems, the first term on the right-hand side of (38) does not exist. On the other hand, during the fission source iteration of the multiplication eigenvalue determination problems, the second term on the right side of (38) vanishes. In either case, (38) represents a linear algebraic system with $N_C + 2N_I$ unknowns but only $N_C + N_I$ equations. Thus a unique solution of (38) would be possible only by augmenting it with a linear system resulting from a BEM discretization of the reflector region.

2.3. BEM discretization of the reflector

For the BEM discretization of the reflector, we divide the boundary of the reflector into a linear boundary element mesh. The nodes which are not on the core-reflector interface are numbered from $i = 1$ to $i = N_R$. On the other hand, the nodes which are on the core-reflector interface are chosen so that they coincide with those on the core (FEM) side. Thus we have exactly N_I nodes on the interface, numbered from $k = 1$ to $k = N_I$ identical to the numbering on the FEM side (see Fig. 3). BEM discretization is based on the choice of the weight function $w(\vec{r})$ in (14) either as the fundamental solution $G_g(\vec{r}, \vec{\rho}_{R,i})(i = 1, \ldots, N_R)$ of the equation:

$$\nabla^2 G_g\left(\vec{r}, \vec{\rho}_{R,i}\right) - \left(k_g^R\right)^2 G_g\left(\vec{r}, \vec{\rho}_{R,i}\right) = -\delta\left(\vec{r} - \vec{\rho}_{R,i}\right) \tag{39}$$

or as the fundamental solution $G_g(\vec{r}, \vec{\rho}_{I,k})(k = 1, \ldots, N_I)$ of the equation:

$$\nabla^2 G_g\left(\vec{r}, \vec{\rho}_{I,k}\right) - \left(k_g^R\right)^2 G_g\left(\vec{r}, \vec{\rho}_{I,k}\right) = -\delta\left(\vec{r} - \vec{\rho}_{I,k}\right), \tag{40}$$

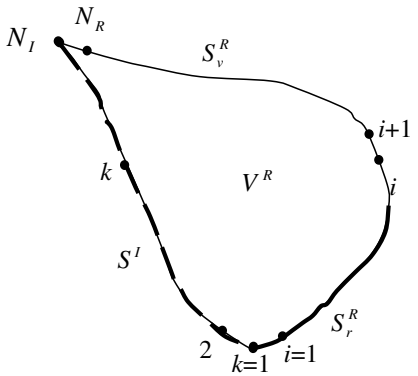

Fig. 3. Boundary element mesh for the reflector.

where $\vec{\rho}_{\mathrm{R},i}$ and $\vec{\rho}_{\mathrm{I},k}$ are the position vectors of the nodes on the non-interface boundary and interface boundary of the reflector respectively. If we take the weight function in (14) as the fundamental solution of (39) and use the integration property of the Dirac delta function, we obtain (Ozgener and Ozgener, 1993):

$$c\left(\vec{\rho}_{\mathrm{R},i}\right)\phi_g\left(\vec{\rho}_{\mathrm{R},i}\right)+\int_{S_r^{\mathrm{R}}}\phi_g(\vec{r})\frac{\partial G_g}{\partial n}\left(\vec{r},\vec{\rho}_{\mathrm{R},i}\right)\mathrm{d}S+\int_{S_v^{\mathrm{R}}}\phi_g(\vec{r})\left[\frac{G_g\left(\vec{r},\vec{\rho}_{\mathrm{R},i}\right)}{2D_g^{\mathrm{R}}}\right.$$
$$\left.+\frac{\partial G_g}{\partial n}\left(\vec{r},\vec{\rho}_{\mathrm{R},i}\right)\right]\mathrm{d}S+\int_{S^{\mathrm{I}}}\left[\phi_g(\vec{r})\frac{\partial G_g}{\partial n}\left(\vec{r},\vec{\rho}_{\mathrm{R},i}\right)+\frac{G_g\left(\vec{r},\vec{\rho}_{\mathrm{R},i}\right)}{2D_g^{\mathrm{R}}}J_g(\vec{r})\right]\mathrm{d}S$$
$$=S_g\left(\vec{\rho}_{\mathrm{R},i}\right)\quad i=1,\ldots,N_{\mathrm{R}},\tag{41}$$

where

$$c\left(\vec{\rho}_{\mathrm{R},i}\right)=\frac{\theta\left(\vec{\rho}_{\mathrm{R},i}\right)}{2\pi},\tag{42}$$

with $\theta(\vec{\rho}_{\mathrm{R},i})$ being the subtended internal angle in radians at the node i. The right-hand side of (41) is given by the volume integral:

$$S_g\left(\vec{\rho}_{\mathrm{R},i}\right)=\int_{V^{\mathrm{R}}}\frac{G_g\left(\vec{r},\vec{\rho}_{\mathrm{R},i}\right)s_g(\vec{r})}{D_g^{\mathrm{R}}}\mathrm{d}V.\tag{43}$$

On the other hand, if we take the weight function in (14) as the fundamental solution of (40) and use the integration property of the Dirac delta function, equations similar to (41)–(43) can be written for the nodes on the core-reflector interface by simply replacing the subscripts "R,i" by "I,k" and "$i=1,\ldots,N_{\mathrm{R}}$" by "$k=1,\ldots,N_{\mathrm{I}}$" in those equations. Since there is no fission source in the reflector and we assume that there is no external neutron source, the only term contributing to the group source term, $s_g(\vec{r})$ in (43) is the scattering source. Since there can be no in-scattering source for the first group, we have:

$$s_g(\vec{r})=\begin{cases}0, & g=1,\\ \Sigma_{\mathrm{s},2\leftarrow1}^{\mathrm{R}}\phi_1(\vec{r}), & g=2,\end{cases}\tag{44}$$

where $\Sigma_{\mathrm{s},2\leftarrow1}^{\mathrm{R}}$ is group 1 to group 2 scattering cross section of the reflector. Thus:

$$S_1\left(\vec{\rho}_{\mathrm{R},i}\right)=0\quad i=1,\ldots,N_{\mathrm{R}}.\tag{45}$$

Hence, for $g=1$, (41) becomes a boundary integral equation (BIE), an integral equation with unknowns only on the reflector boundary. For the second group, the right hand side of (41) could be converted into an expression involving only surface integrals (Ozgener, 1998):

$$S_2\left(\rho_{\mathrm{R},i}\right) = s_{21}\Bigg\{ c\left(\vec{\rho}_{\mathrm{R},i}\right)\phi_1\left(\vec{\rho}_{\mathrm{R},i}\right) + \int_{S_r^{\mathrm{R}}} \phi_1(\vec{r})\,\frac{\partial G_2}{\partial n}\left(\vec{r},\vec{\rho}_{\mathrm{R},i}\right)\mathrm{d}S + \int_{S_v^{\mathrm{R}}} \phi_1(\vec{r})\left[\frac{G_2\left(\vec{r},\vec{\rho}_{\mathrm{R},i}\right)}{2D_1^{\mathrm{R}}} + \frac{\partial G_2}{\partial n}\left(\vec{r},\vec{\rho}_{\mathrm{R},i}\right)\right]\mathrm{d}S + \int_{S^{\mathrm{I}}}\left[\phi_1(\vec{r})\,\frac{\partial G_2}{\partial n}\left(\vec{r},\vec{\rho}_{\mathrm{R},i}\right) + \frac{G_2\left(\vec{r},\vec{\rho}_{\mathrm{R},i}\right)}{D_1^{\mathrm{R}}} J_1(\vec{r})\right]\mathrm{d}S\Bigg\} \quad i = 1,\ldots,N_{\mathrm{R}}, \tag{46}$$

where the group coupling coefficient is

$$s_{21} = \frac{\Sigma_{\mathrm{s},2\leftarrow 1}^{\mathrm{R}}}{D_2^{\mathrm{R}}\left[\left(k_2^{\mathrm{R}}\right)^2 - \left(k_1^{\mathrm{R}}\right)^2\right]}. \tag{47}$$

Equations similar to (45) and (46) are also valid for the nodes on the core-reflector interface. For writing these equations, replacing "R,i" by "I,k" and "$i = 1,\ldots,N_{\mathrm{R}}$" by "$k = 1,\ldots,N_{\mathrm{I}}$" in (45)–(47) will suffice. With (46) inserted into the right-hand side of (41), the second group equation also becomes a BIE. With no volume integrations due to scattering source, the "boundary only" philosophy of BEM is preserved in the reflector equations. Thus, no reflector internal mesh is necessary in the present formulation. Consequently, the first group BIE is

$$c\left(\vec{\rho}_{\mathrm{R},i}\right)\phi_1\left(\vec{\rho}_{\mathrm{R},i}\right) + \int_{S_r^{\mathrm{R}}} \phi_1(\vec{r})\frac{\partial G_1}{\partial n}\left(\vec{r},\vec{\rho}_{\mathrm{R},i}\right)\mathrm{d}S + \int_{S_v^{\mathrm{R}}} \phi_1(\vec{r})\left[\frac{G_1\left(\vec{r},\vec{\rho}_{\mathrm{R},i}\right)}{2D_1^{\mathrm{R}}} + \frac{\partial G_1}{\partial n}\left(\vec{r},\vec{\rho}_{\mathrm{R},i}\right)\right]\mathrm{d}S + \int_{S^{\mathrm{I}}}\left[\phi_1(\vec{r})\frac{\partial G_1}{\partial n}\left(\vec{r},\vec{\rho}_{\mathrm{R},i}\right) + \frac{G_1\left(\vec{r},\vec{\rho}_{\mathrm{R},i}\right)}{D_1^{\mathrm{R}}} J_1(\vec{r})\right]\mathrm{d}S = 0 \quad i = 1,\ldots,N_{\mathrm{R}}. \tag{48}$$

We have an equation in the same form as (48) for the interface nodes $k = 1,\ldots,N_{\mathrm{I}}$. The second group BIE is obtained by using (46) in (41) and can be written as

$$c\left(\vec{\rho}_{\mathrm{R},i}\right)\phi_2\left(\vec{\rho}_{\mathrm{R},i}\right) + \int_{S_r^{\mathrm{R}}} \phi_2(\vec{r})\,\frac{\partial G_2}{\partial n}\left(\vec{r},\vec{\rho}_{\mathrm{R},i}\right)\mathrm{d}S + \int_{S_v^{\mathrm{R}}} \phi_2(\vec{r})\left[\frac{G_2\left(\vec{r},\vec{\rho}_{\mathrm{R},i}\right)}{2D_2^{\mathrm{R}}} + \frac{\partial G_2}{\partial n}\left(\vec{r},\vec{\rho}_{\mathrm{R},i}\right)\right]\mathrm{d}S + \int_{S^{\mathrm{I}}}\left[\phi_2(\vec{r})\,\frac{\partial G_2}{\partial n}\left(\vec{r},\vec{\rho}_{\mathrm{R},i}\right) + \frac{G_2\left(\vec{r},\vec{\rho}_{\mathrm{R},i}\right)}{D_2^{\mathrm{R}}} J_2(\vec{r})\right]\mathrm{d}S$$

$$= s_{21}\left\{ c\left(\vec{\rho}_{\mathrm{R},i}\right)\phi_1\left(\vec{\rho}_{\mathrm{R},i}\right) + \int_{S_r^{\mathrm{R}}} \phi_1(\vec{r})\frac{\partial G_2}{\partial n}\left(\vec{r},\vec{\rho}_{\mathrm{R},i}\right)\mathrm{d}S \right.$$

$$+ \int_{S_v^{\mathrm{R}}} \phi_1(\vec{r})\left[\frac{G_2\left(\vec{r},\vec{\rho}_{\mathrm{R},i}\right)}{2D_1^{\mathrm{R}}} + \frac{\partial G_2}{\partial n}\left(\vec{r},\vec{\rho}_{\mathrm{R},i}\right)\right]\mathrm{d}S$$

$$\left. + \int_{S^{\mathrm{I}}} \left[\phi_1(\vec{r})\frac{\partial G_2}{\partial n}\left(\vec{r},\vec{\rho}_{\mathrm{R},i}\right) + \frac{G_2\left(\vec{r},\vec{\rho}_{\mathrm{R},i}\right)}{D_1^{\mathrm{R}}}J_1(\vec{r})\right]\mathrm{d}S \right\} \quad i = 1,\ldots,N_{\mathrm{R}}. \tag{49}$$

An equation similar to (49) can also be written for $k = 1,\ldots,N_{\mathrm{I}}$. The BIE's (48) and (49) constitute the basic equations for the BEM discretization of the reflector boundary. The linear boundary element trial functions belonging to non-interface nodes i and interface nodes k are denoted by $h_i^{\mathrm{R}}(\vec{r})$ $(i = 1,\ldots,N_{\mathrm{R}})$ and $h_k^{\mathrm{I}}(\vec{r})$ $(k = 1,\ldots,N_{\mathrm{I}})$ respectively. Due to the linearity assumption on both FEM and BEM sides, the finite element and boundary element trial functions are identical on the interface. Before expressing the approximations to the group flux, $\phi_g(\vec{r})$ and current $J_g(\vec{r})$ in (48) and (49), we note that nodes which reside at a junction of S^{R} and S^{I} belong actually to both. But we have counted our junction nodes as interface nodes when we numbered the nodes on the reflector boundary. But in the linear boundary element approximation, the trial functions of such junction nodes also contribute to the flux and current profile on the noninterface part of the reflector boundary. Thus, we must express the approximation to the group flux on S^{R} as

$$\phi_g(\vec{r}) = \left(\underline{\phi}_g^{\mathrm{R}}\right)^{\mathrm{T}}\underline{h}^{\mathrm{R}}(\vec{r}) + \left(\underline{\phi}_g^{\mathrm{I}}\right)^{\mathrm{T}}\underline{h}^{\mathrm{I}}(\vec{r}), \quad \vec{r}\in S^{\mathrm{R}} \tag{50}$$

although the trial function of nonjunction interface nodes actually vanish on S^{R}. Here, the N_{R} and N_{I} dimensional vectors $\underline{\phi}_g^{\mathrm{R}}$ and $\underline{\phi}_g^{\mathrm{I}}$ contain the group flux values at the nodes as their elements. On the other hand, the junction nodes are considered to be part of S^{I}. Thus, we write:

$$\phi_g(\vec{r}) = \left(\underline{\phi}_g^{\mathrm{I}}\right)^{\mathrm{T}}\underline{h}^{\mathrm{I}}(\vec{r}), \quad \vec{r}\in S^{\mathrm{I}}, \tag{51}$$

without any contribution from S^{R} part of the reflector boundary. Since the flux is continuous across the interface $\underline{\phi}_g^{\mathrm{I}}$ vectors defined on the FEM and BEM sides are identical. On the other hand, in both FEM and BEM formulations, the current at the interface is defined as outward directed. But the outward direction for the BEM side is the inward direction for the FEM side. Thus to be consistent with (17) of the FEM formulation and using the continuity of the normal component of current we write:

$$J_g(\vec{r}) = -\left(\underline{J}_g^{\mathrm{I}}\right)^{\mathrm{T}}\underline{h}^{\mathrm{I}}(\vec{r}), \quad \vec{r}\in S^{\mathrm{I}}, \tag{52}$$

so that $\underline{J}_g^{\mathrm{I}}$ represent the current component in the normal direction from the core to the reflector. If we substitute (50)–(52) into the group BIE's of (48) and (49) for non-interface nodes, we obtain the matricial equations:

$$\left(\underline{b}_{1,i}^{\mathrm{R}}\right)^{\mathrm{T}}\underline{\phi}_{1}^{\mathrm{R}}+\left(\underline{b}_{1,i}^{\mathrm{RI}}\right)^{\mathrm{T}}\underline{\phi}_{1}^{\mathrm{I}}+\left(\underline{b}_{1,i}^{\mathrm{RJ}}\right)^{\mathrm{T}}\underline{J}_{1}^{\mathrm{I}}=0,\quad i=1,\ldots,N_{\mathrm{R}} \tag{53}$$

and

$$\left(\underline{b}_{2,i}^{\mathrm{R}}\right)^{\mathrm{T}}\underline{\phi}_{2}^{\mathrm{R}}+\left(\underline{b}_{2,i}^{\mathrm{RI}}\right)^{\mathrm{T}}\underline{\phi}_{2}^{\mathrm{I}}+\left(\underline{b}_{2,i}^{\mathrm{RJ}}\right)^{\mathrm{T}}\underline{J}_{2}^{\mathrm{I}}=s_{21}\left[\left(\underline{b}_{2,i}^{\mathrm{R}}\right)^{\mathrm{T}}\underline{\phi}_{1}^{\mathrm{R}}+\left(\underline{b}_{2,i}^{\mathrm{RI}}\right)^{\mathrm{T}}\underline{\phi}_{1}^{\mathrm{I}}+\left(\underline{b}_{2,i}^{\mathrm{RJ}}\right)^{\mathrm{T}}\underline{J}_{1}^{\mathrm{I}}\right],\quad i=1,\ldots,N_{\mathrm{R}}, \tag{54}$$

where

$$\underline{b}_{g,i}^{\mathrm{R}}=\underline{c}_{i}+\int_{S^{\mathrm{R}}}\underline{h}^{\mathrm{R}}(\vec{r})\frac{\partial G_{g}}{\partial n}\left(\vec{r},\vec{\rho}_{\mathrm{R},i}\right)\mathrm{d}S+\frac{1}{2D_{g}^{\mathrm{R}}}\int_{S_{v}^{\mathrm{R}}}\underline{h}^{\mathrm{R}}(\vec{r})G_{g}\left(\vec{r},\vec{\rho}_{\mathrm{R},i}\right)\mathrm{d}S,\quad i=1,\ldots,N_{\mathrm{R}}, \tag{55}$$

$$\underline{b}_{g,i}^{\mathrm{RI}}=\int_{S^{\mathrm{R}}}\underline{h}^{\mathrm{I}}(\vec{r})\frac{\partial G_{g}}{\partial n}\left(\vec{r},\vec{\rho}_{\mathrm{R},i}\right)\mathrm{d}S+\frac{1}{2D_{g}^{\mathrm{R}}}\int_{S_{v}^{\mathrm{R}}}\underline{h}^{\mathrm{I}}(\vec{r})G_{g}\left(\vec{r},\vec{\rho}_{\mathrm{R},i}\right)\mathrm{d}S,\quad i=1,\ldots,N_{\mathrm{R}}, \tag{56}$$

$$\underline{b}_{g,i}^{\mathrm{RJ}}=-\frac{1}{D_{g}^{\mathrm{R}}}\int_{S^{\mathrm{I}}}\underline{h}^{\mathrm{I}}(\vec{r})G_{g}\left(\vec{r},\vec{\rho}_{\mathrm{R},i}\right)\mathrm{d}S,\quad i=1,\ldots,N_{\mathrm{R}} \tag{57}$$

and

$$\left(\underline{c}_{i}\right)_{j}=\delta_{i,j}c\left(\vec{\rho}_{\mathrm{R},i}\right),\quad i=1,\ldots,N_{\mathrm{R}}. \tag{58}$$

Carrying out same steps for the group BIE's of interface nodes, we obtain the additional matricial equations:

$$\left(\underline{b}_{1,k}^{\mathrm{I}}\right)^{\mathrm{T}}\underline{\phi}_{1}^{\mathrm{I}}+\left(\underline{b}_{1,k}^{\mathrm{IJ}}\right)^{\mathrm{T}}\underline{J}_{1}^{\mathrm{I}}+\left(\underline{b}_{1,k}^{\mathrm{IR}}\right)^{\mathrm{T}}\underline{\phi}_{1}^{\mathrm{R}}=0,\quad k=1,\ldots,N_{\mathrm{I}}, \tag{59}$$

$$\left(\underline{b}_{2,k}^{\mathrm{I}}\right)^{\mathrm{T}}\underline{\phi}_{2}^{\mathrm{I}}+\left(\underline{b}_{2,k}^{\mathrm{IJ}}\right)^{\mathrm{T}}\underline{J}_{2}^{\mathrm{I}}+\left(\underline{b}_{2,k}^{\mathrm{IR}}\right)^{\mathrm{T}}\underline{\phi}_{2}^{\mathrm{R}}=s_{21}\left[\left(\underline{b}_{2,k}^{\mathrm{I}}\right)^{\mathrm{T}}\underline{\phi}_{1}^{\mathrm{I}}+\left(\underline{b}_{2,k}^{\mathrm{IJ}}\right)^{\mathrm{T}}\underline{J}_{1}^{\mathrm{I}}+\left(\underline{b}_{2,k}^{\mathrm{IR}}\right)^{\mathrm{T}}\underline{\phi}_{1}^{\mathrm{R}}\right],\quad k=1,\ldots,N_{\mathrm{I}}, \tag{60}$$

where

$$\underline{b}_{g,k}^{\mathrm{I}}=\underline{c}_{k}+\int_{S^{\mathrm{R}}}\underline{h}^{\mathrm{I}}(\vec{r})\frac{\partial G_{g}}{\partial n}\left(\vec{r},\vec{\rho}_{\mathrm{I},k}\right)\mathrm{d}S+\frac{1}{2D_{g}^{\mathrm{R}}}\int_{S_{v}^{\mathrm{R}}}\underline{h}^{\mathrm{I}}(\vec{r})G_{g}\left(\vec{r},\vec{\rho}_{\mathrm{I},k}\right)\mathrm{d}S,\quad k=1,\ldots,N_{\mathrm{I}}, \tag{61}$$

$$\underline{b}_{g,k}^{\mathrm{IJ}}=-\frac{1}{D_{g}^{\mathrm{R}}}\int_{S^{\mathrm{I}}}\underline{h}^{\mathrm{I}}(\vec{r})G_{g}\left(\vec{r},\vec{\rho}_{\mathrm{I},k}\right)\mathrm{d}S,\quad k=1,\ldots,N_{\mathrm{I}}, \tag{62}$$

$$\underline{b}_{g,k}^{\mathrm{IR}} = \int_{S^{\mathrm{R}}} \underline{h}^{\mathrm{R}}(\vec{r}) \frac{\partial G_g}{\partial n}\left(\vec{r}, \vec{\rho}_{\mathrm{I},k}\right) \mathrm{d}S + \frac{1}{2D_g^{\mathrm{R}}} \int_{S_v^{\mathrm{R}}} \underline{h}^{\mathrm{R}}(\vec{r}) G_g\left(\vec{r}, \vec{\rho}_{\mathrm{I},k}\right) \mathrm{d}S, \quad k = 1, \ldots, N_{\mathrm{I}} \tag{63}$$

and

$$(\underline{c}_k)_j = \delta_{k,j} c\left(\vec{\rho}_{\mathrm{I},k}\right), \quad k = 1, \ldots, N_{\mathrm{I}}. \tag{64}$$

Now we define the matrices $\underline{\underline{B}}_g^{\mathrm{R}}, \underline{\underline{B}}_g^{\mathrm{RI}}$ and $\underline{\underline{B}}_g^{\mathrm{RJ}}$ as matrices whose rows consist of $(\underline{b}_{g,i}^{\mathrm{R}})^{\mathrm{T}}, (\underline{b}_{g,i}^{\mathrm{RI}})^{\mathrm{T}}$ and $(\underline{b}_{g,i}^{\mathrm{RJ}})^{\mathrm{T}}$ for $i = 1, \ldots, N_{\mathrm{R}}$ respectively. Similarly we define the matrices $\underline{\underline{B}}_g^{\mathrm{I}}, \underline{\underline{B}}_g^{\mathrm{IJ}}$ and $\underline{\underline{B}}_g^{\mathrm{IR}}$ as matrices whose rows consist of $(\underline{b}_{g,k}^{\mathrm{I}})^{\mathrm{T}}, (\underline{b}_{g,k}^{\mathrm{IJ}})^{\mathrm{T}}$ and $(\underline{b}_{g,k}^{\mathrm{IR}})^{\mathrm{T}}$ for $k = 1, \ldots, N_{\mathrm{I}}$, respectively. With these definitions (59) and (53) or (60) and (54) could be combined to form the partitioned matrix equation:

$$\begin{bmatrix} \underline{\underline{B}}_g^{\mathrm{I}} & \underline{\underline{B}}_g^{\mathrm{IJ}} & \underline{\underline{B}}_g^{\mathrm{IR}} \\ \underline{\underline{B}}_g^{\mathrm{RI}} & \underline{\underline{B}}_g^{\mathrm{RJ}} & \underline{\underline{B}}_g^{\mathrm{R}} \end{bmatrix} \begin{bmatrix} \underline{\phi}_g^{\mathrm{I}} \\ \underline{J}_g^{\mathrm{I}} \\ \underline{\phi}_g^{\mathrm{R}} \end{bmatrix} = \delta_{g,2} s_{21} \begin{bmatrix} \underline{\underline{B}}_2^{\mathrm{I}} & \underline{\underline{B}}_2^{\mathrm{IJ}} & \underline{\underline{B}}_2^{\mathrm{IR}} \\ \underline{\underline{B}}_2^{\mathrm{RI}} & \underline{\underline{B}}_2^{\mathrm{RJ}} & \underline{\underline{B}}_2^{\mathrm{R}} \end{bmatrix} \begin{bmatrix} \underline{\phi}_1^{\mathrm{I}} \\ \underline{J}_1^{\mathrm{I}} \\ \underline{\phi}_1^{\mathrm{R}} \end{bmatrix} \quad g = 1, 2. \tag{65}$$

The number of unknowns in the linear system of (65) is $2N_{\mathrm{I}} + N_{\mathrm{R}}$; but the number of equations is $N_{\mathrm{I}} + N_{\mathrm{R}}$. The number of unknowns becomes equal to the number of equations only if we combine (38) of FEM formulation with (65) of BEM formulation to get a linear system with $N_{\mathrm{C}} + N_{\mathrm{R}} + 2N_{\mathrm{I}}$ equations and unknowns. The combination of these equations will be discussed in the next subsection.

2.4. Combination of FEM and BEM equations

The FEM equations (38) and BEM equations (65) could be combined by defining the $(N_{\mathrm{C}} + N_{\mathrm{R}} + 2N_{\mathrm{I}})$ dimensional square matrices:

$$\underline{\underline{M}}_g = \begin{bmatrix} \underline{\underline{A}}_g^{\mathrm{C}} & \underline{\underline{A}}_g^{\mathrm{CI}} & \underline{\underline{0}} & \underline{\underline{0}} \\ \left(\underline{\underline{A}}_g^{\mathrm{CI}}\right)^{\mathrm{T}} & \underline{\underline{A}}_g^{\mathrm{I}} & \underline{\underline{A}}_g^{\mathrm{IJ}} & \underline{\underline{0}} \\ \underline{\underline{0}} & \underline{\underline{B}}_g^{\mathrm{I}} & \underline{\underline{B}}_g^{\mathrm{IJ}} & \underline{\underline{B}}_g^{\mathrm{IR}} \\ \underline{\underline{0}} & \underline{\underline{B}}_g^{\mathrm{RI}} & \underline{\underline{B}}_g^{\mathrm{RJ}} & \underline{\underline{B}}_g^{\mathrm{R}} \end{bmatrix}, \tag{66}$$

$$\underline{\underline{F}}_{g \leftarrow g'} = \begin{bmatrix} \underline{\underline{F}}_{g \leftarrow g'}^{\mathrm{C}} & \underline{\underline{F}}_{g \leftarrow g'}^{\mathrm{CI}} & \underline{\underline{0}} & \underline{\underline{0}} \\ \left(\underline{\underline{F}}_{g \leftarrow g'}^{\mathrm{CI}}\right)^{\mathrm{T}} & \underline{\underline{F}}_{g \leftarrow g'}^{\mathrm{I}} & \underline{\underline{0}} & \underline{\underline{0}} \\ \underline{\underline{0}} & \underline{\underline{0}} & \underline{\underline{0}} & \underline{\underline{0}} \\ \underline{\underline{0}} & \underline{\underline{0}} & \underline{\underline{0}} & \underline{\underline{0}} \end{bmatrix}, \tag{67}$$

$$\underline{\underline{S}}_{2\leftarrow 1} = \begin{bmatrix} \underline{\underline{S}}^{C}_{2\leftarrow 1} & \underline{\underline{A}}^{CI}_{2\leftarrow 1} & \underline{\underline{0}} & \underline{\underline{0}} \\ \left(\underline{\underline{S}}^{CI}_{2\leftarrow 1}\right)^{T} & \underline{\underline{S}}^{I}_{2\leftarrow 1} & \underline{\underline{0}} & \underline{\underline{0}} \\ \underline{\underline{0}} & s_{21}\underline{\underline{B}}^{I}_{2} & s_{21}\underline{\underline{B}}^{IJ}_{2} & s_{21}\underline{\underline{B}}^{IR}_{2} \\ \underline{\underline{0}} & s_{21}\underline{\underline{B}}^{RI}_{2} & s_{21}\underline{\underline{B}}^{RJ}_{2} & s_{21}\underline{\underline{B}}^{R}_{2} \end{bmatrix}, \tag{68}$$

and $(N_C + N_R + 2N_I)$ dimensional vectors:

$$\underline{u}_g^{T} = \begin{bmatrix} \left(\underline{\phi}_g^{C}\right)^{T} & \left(\underline{\phi}_g^{I}\right)^{T} & \left(\underline{J}_g^{I}\right)^{T} & \left(\underline{\phi}_g^{R}\right)^{T} \end{bmatrix}, \tag{69}$$

$$\underline{f}_g^{T} = \begin{bmatrix} \left(\underline{s}_g^{C}\right)^{T} & \left(\underline{s}_g^{I}\right)^{T} & \underline{0} & \underline{0} \end{bmatrix}. \tag{70}$$

The two-group equations can be written even more compactly, by defining the block matrices:

$$\underline{\underline{M}} = \begin{bmatrix} \underline{\underline{M}}_1 & \underline{\underline{0}} \\ -\underline{\underline{S}}_{2\leftarrow 1} & \underline{\underline{M}}_2 \end{bmatrix}, \tag{71}$$

$$\underline{\underline{F}} = \begin{bmatrix} \underline{\underline{F}}_{1\leftarrow 1} & \underline{\underline{F}}_{1\leftarrow 2} \\ \underline{\underline{F}}_{2\leftarrow 1} & \underline{\underline{F}}_{2\leftarrow 2} \end{bmatrix} \tag{72}$$

and block-vectors:

$$\underline{u}^{T} = \begin{bmatrix} \underline{u}_1^{T} & \underline{u}_2^{T} \end{bmatrix}, \tag{73}$$

$$\underline{f}^{T} = \begin{bmatrix} \underline{f}_1^{T} & \underline{f}_2^{T} \end{bmatrix}. \tag{74}$$

With these definitions, the two-group external source problem is represented by the matricial equation:

$$\underline{\underline{M}}\underline{u} = \underline{f}, \tag{75}$$

which can be solved by solving the linear systems:

$$\underline{\underline{M}}_1\underline{u}_1 = \underline{f}_1, \tag{76}$$

and

$$\underline{\underline{M}}_2\underline{u}_2 = \underline{f}_2 + \underline{\underline{S}}_{2\leftarrow 1}\underline{u}_1, \tag{77}$$

consecutively. For fission source iteration problems, we have to solve the linear system:

$$\underline{\underline{M}}\underline{u}^{(n)} = \underline{f}^{(n)}, \tag{78}$$

at the n'th iteration, where:

$$\underline{f}^{(n)} = \frac{1}{k^{(n-1)}}\underline{\underline{F}}\underline{u}^{(n-1)}, \tag{79}$$

where $k^{(n-1)}$ and $\underline{u}^{(n-1)}$ are known from the previous iteration. (78) can again be solved by solving the counterparts of (76) and (77). For one group external source or fission source iteration problems, the solution algorithm is shortened. The step given in (77) is absent.

3. Implementation and validation

The developed FE/BE hybrid method is implemented in the FORTRAN program NEDPCM. The program is capable of handling one and two group diffusion theory problems of the external source and multiplication factor (k_{eff}) determination variety. The program is developed and tested in PC environments under the MS WINDOWS operating systems using the MS FORTRAN platform.

The first problem we consider is a one-group external neutron source problem involving a bare system consisting of a square core of side length a surrounded by a reflector of thickness b from the left and right but not from the top and bottom. Due to the symmetry, only the upper right quadrant of the system is discretized. Reflection boundary conditions on the left and bottom sides of the upper right quadrant are utilized to impose the symmetry of the full system. Vacuum boundary condition prevails naturally at the top and right sides of the bare system. A geometrical description of the upper right quadrant of the system which is to be discretized is presented in Fig. 4. The governing one-group diffusion equations of the core and reflector are:

$$-D\nabla^2\phi(\vec{r}) + \Sigma_a\phi(\vec{r}) = s, \quad \vec{r} \in V^C, \tag{80}$$

$$-D\nabla^2\phi(\vec{r}) + \Sigma_a\phi(\vec{r}) = 0, \quad \vec{r} \in V^R, \tag{81}$$

with the diffusion constant D and the absorption cross section Σ_a of the core and the reflector taken equal for ease of analytical solution. A uniform external neutron source of magnitude, s, is assumed to be present in the core. On the other hand, the reflector is assumed to contain no external neutron source. Since there is only one group, the group indices g in (1) are dropped in (80) and (81). Since the one-group absorption cross section (Σ_a) is equal to the one-group removal cross section, Σ_r of (1) is replaced by Σ_a in (80) and (81). Eqs. (80) and (81) have been solved analytically

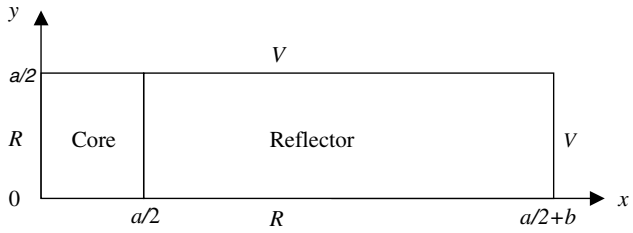

Fig. 4. Geometrical description of the upper-right quadrant of the partially reflected system.

and the analytically derived expressions for the core and reflector average fluxes denoted by $\bar{\phi}_C$ and $\bar{\phi}_R$ respectively, are presented below:

$$\bar{\phi}_C = \frac{sf(ka/2)}{\Sigma_a}\left[1 + \frac{\sinh(\beta a/2)}{(\beta a/2)} g(\eta, \beta a/2)\right], \tag{82}$$

$$\bar{\phi}_R = \frac{sf(ka/2)}{\Sigma_a}[1 + \cosh(\beta a/2) g(\eta, \beta a/2)] h(a, b, t, \beta), \tag{83}$$

where the functions f, g, and h are defined as

$$f(ka/2) = 1 - \frac{\sinh(ka/2)}{(ka/2)[\cosh(ka/2) + 2kD\sinh(ka/2)]}, \tag{84}$$

$$g(\eta, \beta a/2) = \frac{\eta}{\sinh(\beta a/2) - \eta\cosh(\beta a/2)}, \tag{85}$$

$$h(a,b,t,\beta) = \frac{\cosh[\beta(a/2+b)] - \cosh(\beta a/2) - t\{\sinh[\beta(a/2+b)] - \sinh(\beta a/2)\}}{(\beta b)[\sinh(\beta a/2) - t\cosh(\beta a/2)]}. \tag{86}$$

The factor η and the coupling coefficient t are defined as

$$\eta = \frac{\cosh(\beta a/2) - t\sinh(\beta a/2)}{\sinh(\beta a/2) - t\cosh(\beta a/2)}, \tag{87}$$

$$t = \frac{\sinh[\beta(a/2+b)] + 2\beta D\cosh[\beta(a/2+b)]}{\cosh[\beta(a/2+b)] + 2\beta D\sinh[\beta(a/2+b)]}. \tag{88}$$

The constant β has the definition:

$$\beta = \sqrt{k^2 + \gamma^2}, \tag{89}$$

where γ is the smallest positive root of the transcendental equation:

$$\gamma\tan(\gamma a/2) = \frac{1}{2D}. \tag{90}$$

The one-group external source problem has been run with various FE/BE hybrid meshes using our program NEDPCM. In general, the core is divided into N_{xC} and N_y equal parts in the x and y-directions respectively so that a bilinear rectangular finite element mesh with $N_{xC} \times N_y$ elements is superimposed on the core. Such a mesh is denoted as a $N_{xC} \times N_y$ mesh for the core. With a $N_{xC} \times N_y$ FEM mesh, $N_C = N_{xC}(N_y + 1)$ and $N_I = N_y + 1$. The reflector is divided into N_y linear boundary elements on both the interface side and the right side which is parallel to the interface. The bottom and top sides of the reflector is divided into N_{xR} linear boundary elements. Such a reflector BEM mesh is called a $N_{xR} \times N_y$ mesh. For such a BEM mesh $N_R = 2N_{xR} + N_y - 1$. A hybrid mesh consisting of a $(N_{xC} \times N_y)$ FEM and $(N_{xR} \times N_y)$ BEM mesh with the associated node numbering system is presented in Fig. 5 for the case $N_{xC} = 2$, $N_y = 3$ and $N_{xR} = 4$.

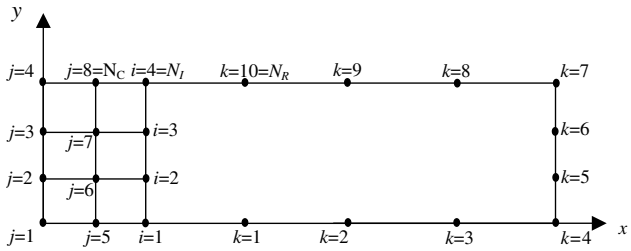

Fig. 5. The (2×3) FEM, (4×3) BEM hybrid mesh used by NEDPCM.

Table 1
Average fluxes for the one-group external source problem

Hybrid mesh		$\bar{\phi}_C$ (cm^{-1} s^{-1})	$\bar{\phi}_R$ (cm^{-1} s^{-1})	$\bar{\phi}$ (cm^{-1} s^{-1})
Core (FEM)	Reflector (BEM)			
2×2	2×2	6.62223 (3.12%)	1.50636 (28.8%)	2.50649 (10.07%)
5×4	5×4	6.81101 (0.36%)	1.23355 (5.47%)	2.32391 (2.05%)
10×8	10×8	6.83616 (0.01%)	1.18594 (1.40%)	2.29053 (0.59%)
20×16	20×16	6.84024 (0.07%)	1.17267 (0.27%)	2.28065 (0.15%)
Analytical		6.83531	1.16954	2.27717

NEDPCM runs have been made for this one group external source problem with various hybrid meshes and the following data: $D = 1.77764$ cm, $\Sigma_a = 0.0143676$ cm^{-1}, $a/2 = 4.86$ cm, $b = 20$ cm, $s = 1$ neutron/(cm^3 s). The average core flux $\bar{\phi}_C$, the average reflector flux, $\bar{\phi}_R$ and the average flux ($\bar{\phi} = x_C\bar{\phi}_C + x_R\bar{\phi}_R$, where the volume fractions are defined as $x_C = a^2/[a(a+2b)]$ and $x_R = 1 - x_C$) obtained with various hybrid meshes along with their analytical values are presented in Table 1. The per cent errors of various runs relative to the analytical values are also given in parentheses. The average fluxes are seen to converge to the analytical values as the meshes are refined. The pointwise flux distributions along $y = 0$, obtained both analytically and numerically (20×16 hybrid mesh) are presented in Fig. 6. The two graphs are not discernable due to the high accuracy in the numerical solution.

The second problem we consider is again a one-group problem that involves multiplication eigenvalue (k_{eff}) determination. We assume again a bare system with a square core of sidelength a and a reflector of thickness b surrounding the core from left and right. Again, the upper-right quadrant of the system is properly represented by Fig. 4. The governing one-group diffusion equation for the core and reflector are:

$$-D\nabla^2\phi(\vec{r}) + \Sigma_a^C\phi(\vec{r}) = \frac{1}{k_{eff}}\upsilon\Sigma_f^C\phi(\vec{r}), \quad \vec{r} \in V^C, \tag{91}$$

$$-D\nabla^2\phi(\vec{r}) + \Sigma_a^R\phi(\vec{r}) = 0, \quad \vec{r} \in V^R. \tag{92}$$

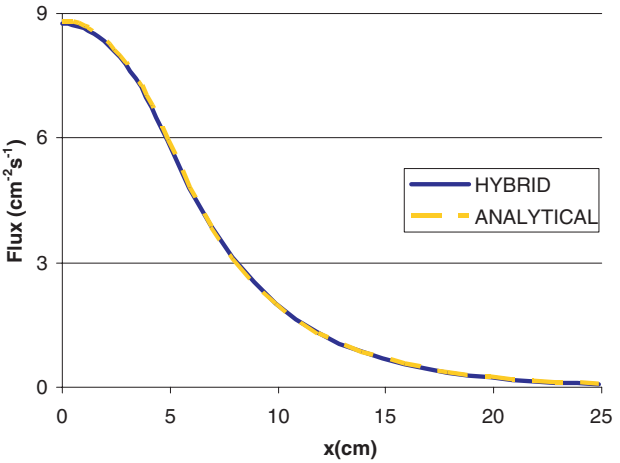

Fig. 6. Flux profile along $y = 0$ for the one group external source problem.

The diffusion constant of the core and reflector are taken equal to D for the ease of analytical solution. The problem is to be solved for the largest eigenvalue, k_{eff}, and the corresponding nonnegative eigenfunction, the neutron flux, $\phi(\vec{r})$. This problem is solved numerically by fission source iteration in NEDPCM. This eigenvalue–eigenvector problem has been solved analytically and the multiplication eigenvalue (k_{eff}) is given by

$$k_{\text{eff}} = \frac{(\upsilon\Sigma_{\text{f}}^{\text{C}}/\Sigma_{\text{a}}^{\text{C}})}{1 + B_m^2/(k^{\text{C}})^2}, \tag{93}$$

where

$$B_m^2 = B_x^2 + B_y^2, \tag{94}$$

B_y and B_x are the smallest positive roots of the transcendental equations:

$$B_y \tan\left(B_y a/2\right) = \frac{1}{2D}, \tag{95}$$

$$B_x \tan\left(B_x a/2\right) = -\beta \frac{\cosh\left(\beta a/2\right) - t\sinh\left(\beta a/2\right)}{\sinh\left(\beta a/2\right) - t\cosh\left(\beta a/2\right)}, \tag{96}$$

where

$$\beta = \sqrt{B_y^2 + (k^{\text{R}})^2} \tag{97}$$

and

$$t = \frac{\sinh\left[\beta(a/2+b)\right] + 2\beta D\cosh\left[\beta(a/2+b)\right]}{\cosh\left[\beta(a/2+b)\right] + 2\beta D\sinh\left[\beta(a/2+b)\right]}. \tag{98}$$

When the thermal power per unit distance of the nuclear system and the energy released per fission are denoted by P' and w_f respectively, the flux distribution is analytically found as

$$\phi(x,y)=\begin{cases}\dfrac{P'B_xB_y}{4w_f\Sigma_f^C\sin(B_xa/2)\sin(B_ya/2)}\cos(B_xx)\cos(B_yy),\\ \quad 0<x<a/2,0<y<a/2,\\ \left\{\dfrac{P'B_xB_y}{4w_f\Sigma_f^C\tan(B_xa/2)\sin(B_ya/2)[\sinh(\beta a/2)-t\cosh(\beta a/2)]}\right\}\\ \{[\sinh(\beta x)-t\cosh(\beta x)]\cos(B_yy)\},\\ \quad a/2<x<a/2+b,0<y<a/2.\end{cases}\tag{99}$$

This problem is also solved by a finite element neutron diffusion program FEND (Ozgener and Kabadayı, 1996). Finite element meshes used by FEND are also represented by the notation $(N_{xC}\times N_y)$, $(N_{xR}\times N_y)$. The first parenthesis still preserves its original meaning; the second parenthesis describes a bilinear rectangular finite element mesh consisting of $N_{xR}\times N_y$ elements superimposed on the reflector region. An example of FEM mesh used by FEND is given in Fig. 7. While the FEM mesh of Fig. 7 contains a total of 28 nodes (unknowns); its hybrid equivalent of Fig. 5 contains a total of 22 nodes; but 26 unknowns since each node on the interface has two unknowns associated with it. For this problem, we have taken $D=0.87$ cm, $\Sigma_a^C=0.01122\ \text{cm}^{-1}$, $\Sigma_a^R=0.0033\ \text{cm}^{-1}$, $\upsilon\Sigma_f^C=0.0230452\ \text{cm}^{-1}$, $\Sigma_f^C=0.0921808\ \text{cm}^{-1}$, $a/2=22.5$ cm, $b=20$ cm. In Table 2, the k_{eff} values calculated by the programs NEDPCM (hybrid) and FEND (FEM) with various meshes are presented. The number of unknowns (N_{tot}) (which is equal to the dimension of resulting linear system) is also given for each mesh and method. The values in parenthesis under k_{eff} values give the per cent error relative to the analytical value of $k_{\text{eff}}=1.361959$.

The multiplication eigenvalues calculated by both the hybrid method and FEM seems to converge to the analytical k_{eff} as the meshes are refined. For equivalent meshes, the per cent errors generated by the hybrid method are a little bit smaller than those generated by FEM. The dimension of the linear system generated by the hybrid method is smaller than the one generated by the use of the equivalent FEM mesh. Only in the coarsest mesh, the $((5\times3),(3\times3))$ mesh, the linear system

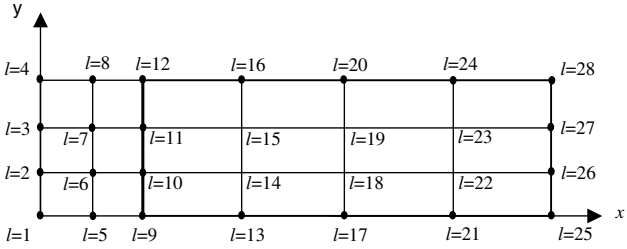

Fig. 7. The (2×3) core, (4×3) reflector finite element mesh used by FEND.

Table 2
k_{eff} values for the one-group, multiplication eigenvalue problem

Mesh		Method			
Core mesh	Reflector mesh	Hybrid		FEM	
		N_{tot}	k_{eff}	N_{tot}	k_{eff}
5×3	3×3	36	1.354105 (0.58%)	36	1.353971 (0.59%)
5×5	3×5	52	1.358929 (0.22%)	54	1.357959 (0.29%)
10×6	6×6	101	1.360011 (0.14%)	119	1.359964 (0.15%)
10×10	6×10	153	1.361227 (0.05%)	187	1.360955 (0.07%)

dimension generated by both methods are equal. The ratio of the linear system dimension of FEM to that of the hybrid method increases as the mesh is refined. This is expected since the large number of internal reflector nodes is not present in the hybrid formulation. Taking $P' = 4000$ W/cm and $w_f = 3.2044 \times 10^{-11}$ Joule/fission, the average core and reflector fluxes are also calculated. The analytical values of the average core flux ($\bar{\phi}_C$) and average reflector flux ($\bar{\phi}_R$) found by integration of (98) are 2.67493×10^{13} cm^{-2} s^{-1} and $6.33803 \times {}^{12}$ cm^{-2} s^{-1}, respectively. The average core fluxes calculated by the hybrid method and FEM are almost equal to the analytical value for all meshes given in Table 2 and have zero error for all practical purposes. The average reflector flux values calculated by both the hybrid method and FEM are given in Table 3. The per cent errors compared to the analytical value are also given in parentheses there. Per cent errors in reflector fluxes seem to be depending basically on the number of nodes used on the top and bottom sides of the reflector. Increasing the number of nodes on the left and right sides do not increase the accuracy. Moreover, they seem to decrease the accuracy a little bit. This behavior is observed in both hybrid and FEM results. For the reflector average flux, FEM errors are slightly smaller than the ones generated by the hybrid method in contrast to the situation in k_{eff} comparison.

The third problem, we'll dwell on is a two-group external neutron source problem again involving a bare system with a square core of sidelength a with a reflector of thickness b surrounding the core from left and right. Thus, only the upper-right

Table 3
Average reflector fluxes in units of 10^{12} cm^{-2} s^{-1} for the one-group multiplication eigenvalue problem

Mesh	Core Reflector	5×3 3×3	5×5 3×5	10×6 6×6	10×10 6×10
Hybrid		6.47408 (2.15%)	6.53696 (3.14%)	6.37137 (0.53%)	6.38864 (0.80%)
FEM		6.45055 (1.78%)	6.46759 (2.04%)	6.36583 (0.44%)	6.37008 (0.51%)

quadrant (as given in Fig. 4) is to be discretized. The boundary conditions are taken to be the same as those in the first problem. But they apply to both groups this time. We assume there is no external source in the reflector and there is a uniform neutron source in the core for both groups: $s_1(\vec{r}) = s_1$, $s_2(\vec{r}) = s_2$, $\vec{r} \in V^{\mathrm{C}}$; $s_1(\vec{r}) = 0$, $s_2(\vec{r}) = 0$, $\vec{r} \in V^{\mathrm{R}}$. The diffusion constants of both groups and both regions are taken to be the same and equal to D for ease of analytical solution. The flux distribution for this problem has also been determined analytically as follows:

$$\phi_1(x,y) = \begin{cases} A\cosh(\beta_1 x)\cos(\gamma y) + \frac{s_1}{\Sigma^{\mathrm{C}}_{\mathrm{r},1}}\left[1 - \xi_1 \cosh\left(k_1^{\mathrm{C}} y\right)\right], \\ \quad 0 < x < a/2, \;\; 0 < y < a/2, \\ E'[\cosh(\mu_1 x) - t_1 \sinh(\mu_1 x)]\cos(\gamma y), \\ \quad a/2 < x < a/2 + b, \;\; 0 < y < a/2, \end{cases} \tag{100}$$

$$\phi_2(x,y) = \begin{cases} \cos(\gamma y)\left[F\cosh(\beta_2 x) + s^{\mathrm{C}}_{21} A \cosh(\beta_1 x)\right] \\ +s^{\mathrm{C}}_{21}\frac{s_1}{\Sigma^{\mathrm{C}}_{\mathrm{r},1}}\left[\xi_2 \cosh\left(k_2^{\mathrm{C}} y\right) - \xi_1 \cosh\left(k_1^{\mathrm{C}} y\right)\right] + \rho\left[1 - \xi_2 \cosh\left(k_2^{\mathrm{C}} y\right)\right], \\ \quad 0 < x < a/2, \;\; 0 < y < a/2, \\ \left\{F'[\cosh(\mu_2 x) - t_2 \sinh(\mu_2 x)]\right. \\ \left. + E' s_{21}[\cosh(\mu_1 x) - t_1 \sinh(\mu_1 x)]\right\}\cos(\gamma y), \\ \quad a/2 < x < a/2 + b, \;\; 0 < y < a/2, \end{cases} \tag{101}$$

where γ is the smallest positive root of the transcendental equation:

$$\gamma \tan\gamma = \frac{1}{2D}. \tag{102}$$

The coefficients β_g and μ_g ($g = 1, 2$) are defined in terms of γ as

$$\beta_g^2 = \gamma^2 + \left(k_g^{\mathrm{C}}\right)^2, \qquad \mu_g^2 = \gamma^2 + \left(k_g^{\mathrm{R}}\right)^2.$$

The coupling coefficients, t_g of the reflector and the constant ξ_g of the core are defined for $g = 1$ or 2 as

$$t_g = \frac{\cosh\left[\mu_g(a/2 + b)\right] + 2D\mu_g \sinh\left[\mu_g(a/2 + b)\right]}{\sinh\left[\mu_g(a/2 + b)\right] + 2D\mu_g \cosh\left[\mu_g(a/2 + b)\right]}, \tag{103}$$

$$\xi_g = \frac{1}{\cosh\left(k_g^{\mathrm{C}} a/2\right) + 2Dk_g^{\mathrm{C}} \sinh\left(k_g^{\mathrm{C}} a/2\right)}. \tag{104}$$

The factor A of the first equation in (100) is given in terms of the previously defined quantities as

$$A = \frac{\mu_1 s_1 \delta_1\left[\xi_1 \cosh(k_1^{\mathrm{C}} y) - 1\right]}{\Sigma^{\mathrm{C}}_{\mathrm{r},1}\cos(\gamma y)[\mu_1\delta_1\cos(\beta_1 a/2) - \beta_1\eta_1\sin(\beta_1 a/2)]}, \tag{105}$$

where

$$\delta_g = \sinh\left(\mu_g a/2\right) - t_g \cosh\left(\mu_g a/2\right), \tag{106}$$

$$\eta_g = \cosh\left(\mu_g a/2\right) - t_g \sinh\left(\mu_g a/2\right). \tag{107}$$

The factor E' of the second equation in (100) is defined in terms of A as

$$E' = \frac{1}{\eta_1}\left\{ A\cosh\left(\beta_1 a/2\right) + \frac{s_1\left[1-\xi_1\cosh\left(k_1^{\mathrm{C}} y\right)\right]}{\Sigma_{\mathrm{r},1}^{\mathrm{C}}\cos\left(\gamma y\right)} \right\}. \tag{108}$$

The factor s_{21}^{C} which appears in the first equation of (101) is the group-to-group coupling coefficient of the core and is defined similarly to the reflector group-to-group coefficient s_{21} of (47) as

$$s_{21}^{\mathrm{C}} = \frac{\Sigma_{\mathrm{s},2\leftarrow 1}^{\mathrm{C}}}{D_2\left[\left(k_2^{\mathrm{C}}\right)^2 - \left(k_1^{\mathrm{C}}\right)^2\right]}, \tag{109}$$

ρ of the first equation of (100) is another factor characterizing group coupling in the core and is defined as

$$\rho = \frac{1}{\Sigma_{\mathrm{a},2}^{\mathrm{C}}}\left[\frac{\Sigma_{\mathrm{s},2\leftarrow 1}^{\mathrm{C}}}{\Sigma_{\mathrm{r},1}} s_1 + s_2\right]. \tag{110}$$

The factor F' of the second equation in (101) is given as

$$\begin{aligned} F' = {} & \frac{E' s_{21}\mu_1\delta_1 - A s_{21}^{\mathrm{C}}\beta_1\sin\left(\beta_1 a/2\right)}{\beta_2\eta_2\tanh\left(\beta_2 a/2\right) - \mu_2\delta_2} - \frac{\beta_2\tanh\left(\beta_2 a/2\right)}{\beta_2\eta_2\tanh\left(\beta_2 a/2\right) - \mu_2\delta_2}\left\{ E' s_{21}\eta_1 \right. \\ & - A s_{21}^{\mathrm{C}}\cosh\left(\beta_1 a/2\right) - \frac{s_{21}^{\mathrm{C}} s_1\left[\xi_2\cosh\left(k_2^{\mathrm{C}} y\right) + \xi_1\cosh\left(k_1^{\mathrm{C}} y\right)\right]}{\Sigma_{\mathrm{r},1}^{\mathrm{C}}\cos\left(\gamma y\right)} \\ & \left. - \frac{\rho\left[1-\xi_2\cosh\left(k_{21}^{\mathrm{C}} y\right)\right]}{\cos\left(\gamma y\right)} \right\}. \end{aligned} \tag{111}$$

The factor F is simply:

$$F = -t_2 F'. \tag{112}$$

We've run this problem with NEDPCM assuming that the core and the reflector are made of the same material. Thus the two-group constants for both regions are identical. We assume $s_1 = 1\ \mathrm{cm}^{-1}$, $s_2 = 1\ \mathrm{cm}^{-1}$ in the core and zero in the reflector. The dimensions $a/2 = 4.86$ cm, $b = 20$ cm are again assumed. The first and second group diffusion constants are again assumed to be equal for both groups to render the analytical solution possible. The cross section data is $D = 0.6450$ cm, $\Sigma_{\mathrm{r},1} = 0.0494\ \mathrm{cm}^{-1}$, $\Sigma_{\mathrm{a},2} = 0.0197\ \mathrm{cm}^{-1}$, $\Sigma_{\mathrm{s},2\leftarrow 1} = 0.0490\ \mathrm{cm}^{-1}$. NEDPCM runs have been made for this two-group external source problem with various hybrid meshes. The average core group fluxes $\bar{\phi}_{\mathrm{C}}^1, \bar{\phi}_{\mathrm{C}}^2$ and the average reflector fluxes $\bar{\phi}_{\mathrm{R}}^1, \bar{\phi}_{\mathrm{R}}^2$ obtained with various hybrid meshes along with the analytical values are presented in Table 4. The per cent errors of various runs relative to the analytical values are also

Table 4
Average fluxes for the two-group external source problem

Hybrid mesh		$\bar{\phi}^1_C$ (cm^{-2} s^{-1})	$\bar{\phi}^1_R$ (cm^{-2} s^{-1})	$\bar{\phi}^2_C$ (cm^{-2} s^{-1})	$\bar{\phi}^2_R$ (cm^{-2} s^{-1})
Core (FEM)	Reflector (BEM)				
5×4	5×4	7.490883 (0.30%)	0.777711 (18.02%)	14.820345 (0.67%)	2.094908 (7.31%)
10×8	10×8	7.525357 (0.16%)	0.688016 (4.41%)	14.930841 (0.07%)	1.985079 (1.68%)
10×8	20×8	7.521299 (0.11%)	0.662078 (0.47%)	14.928408 (0.05%)	1.950161 (0.11%)
Analytical		7.513168	0.65898	14.920575	1.95224

Table 5
Cross section data for the two-group criticality eigenvalue problem

	$\Sigma^j_{r,1}$	$\Sigma^j_{r,2}$	$\upsilon\Sigma^j_{f,1}$	$\upsilon\Sigma^j_{f,2}$	$\Sigma^j_{s,2\leftarrow1}$
Core ($j = C$)	0.080117	0.11484	0.0813	0.17843	0.063567
Reflector ($j = R$)	0.01021	0.00267	0	0	0.01005

given in parentheses. The average group fluxes, both in the core and reflector approach the analytical values as the hybrid meshes are refined. The reflector average fluxes seem to depend on the number of BEM nodes used on the bottom and top sides of the reflector.

The last case, we'll consider is the two-group, multiplication eigenvalue (k_{eff}) determination problem. The upper-right quadrant of the system is again as described in Fig. 4. The two-group cross sections used for this problem are presented in Table 5 in units of cm^{-1}. To render analytical solution possible, the diffusion constants of both group and both regions are taken to be equal. That is $D = D^{\text{C}}_1 = D^{\text{C}}_2 = D^{\text{R}}_1 = D^{\text{R}}_2 = 0.6165356$ cm. We have also $\chi_1 = 1$, $\chi_2 = 0$. The geometrical data is again: $a/2 = 4.86$ cm, $b = 20$ cm. The analytical solution of this problem is given in Ozgener and Ozgener (2001). This problem has been run with various hybrid meshes using NEDPCM. For comparison, we have included the results obtained by the constant BEM program, namely GLOBAL (Ozgener and Ozgener, 2001). Boundary element meshes used by GLOBAL are denoted again by the notation ($N_{xC} \times N_y$), ($N_{xR} \times N_y$). Since GLOBAL is a constant boundary element program, each constant boundary element contains just one node which is in its geometric center. N_{xC} and N_{xR} represent the number of constant boundary elements on the top (or bottom) sides of the core and reflector respectively. N_y is the number of constant boundary elements on the left and right sides of the core and reflector. A (2×3) core (4×3) reflector constant boundary element mesh represented in Fig. 8. A ($N_{xC} \times N_y$), ($N_{xR} \times N_y$) constant BEM mesh introduces a total of 2 $(N_{xC} + N_{xR}) + 3N_y$ nodes or $2(N_{xC} + N_{xR}) + 4N_y$ unknowns per group since N_y nodes on the core-reflector interface have two unknowns (flux and current) associated with each. In Table 6, the k_{eff}

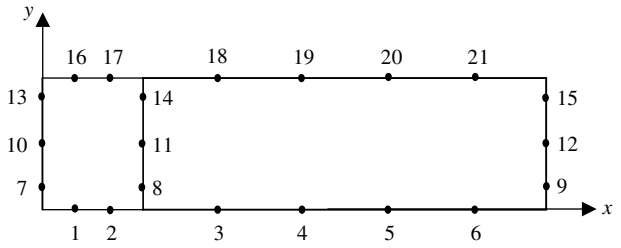

Fig. 8. The (2×3) core, (4×3) reflector constant boundary element mesh used by GLOBAL.

Table 6
k_{eff} values for the two group multiplication eigenvalue problem

Method	Mesh	N_{tot}	k_{eff}
Hybrid	$(5 \times 4)(5 \times 4)$	48	0.99454 (0.55%)
CBEM	$(4 \times 4)(5 \times 4)$	34	0.97826 (2.17%)
Hybrid	$(10 \times 8)(10 \times 8)$	135	0.99892 (0.11%)
CBEM	$(8 \times 8)(10 \times 8)$	68	0.99288 (0.71%)
Hybrid	$(20 \times 16)(20 \times 16)$	429	0.99977 (0.02%)
CBEM	$(16 \times 16)(20 \times 16)$	136	0.99781 (0.22%)
CBEM	$(32 \times 32)(40 \times 32)$	272	0.99907 (0.09%)

values obtained by various meshes by the hybrid method and constant BEM are presented. The per cent errors relative to the analytical $k_{\text{eff}} = 1$ are also given underneath in parenthesis. The number of unknowns per energy group (N_{tot}) associated with each run is also given. Both the FE/BE hybrid and constant boundary element methods (CBEM) approach the analytical k_{eff} as the mesh is refined. With equal number of unknowns per group, the per cent error associated with the hybrid FE/BE method is smaller than that associated with the constant boundary element solution. Perhaps a better comparison could have been made with a pure linear boundary element solution. Since our multiregion BEM code (GLOBAL) handles only constant boundary elements, such a comparison could not have been carried out. With P', (thermal reactor power per unit distance) taken as 4000 W/cm and $\Sigma^{\text{C}}_{\text{f},1} = 0.03252$ cm^{-1}, $\Sigma^{\text{C}}_{\text{f},2} = 0.071372$ cm^{-1}, the average core and reflector group fluxes, calculated analytically by the hybrid method with various meshes are presented in Table 7.

Table 7
Regionwise average group fluxes calculated by the hybrid method for the two-group multiplication eigenvalue problem

Mesh	$\bar{\phi}^{\text{C}}_1$ (10^{-13} cm^{-2} s^{-1})	$\bar{\phi}^{\text{R}}_1$ (10^{-13} cm^{-2} s^{-1})	$\bar{\phi}^{\text{C}}_2$ (10^{-13} cm^{-2} s^{-1})	$\bar{\phi}^{\text{R}}_2$ (10^{-13} cm^{-2} s^{-1})
$(5 \times 4)(5 \times 4)$	9.0484 (0.21%)	1.1547 (10.71%)	3.2820 (0.27%)	5.7062 (2.36%)
$(10 \times 8)(10 \times 8)$	9.0337 (0.05%)	1.0729 (2.87%)	3.2887 (0.06%)	5.6127 (0.68%)
$(20 \times 16)(20 \times 16)$	9.0303 (0.01%)	1.0508 (0.75%)	3.2903 (0.02%)	5.5855 (0.19%)
Analytical	9.0292	1.0430	3.2908	5.5748

These results also show the convergence to the analytical values when the mesh is refined.

4. Conclusions and recommendations

A hybrid formulation involving a FEM mesh for the reactor core and BEM mesh for the reflector has been developed, implemented and validated. Comparisons with pure FEM and BEM codes have shown that the hybrid method constitutes a viable alternative to these methods. In the current implementation of the hybrid method, the linear system obtained by combining the FEM and BEM equations are stored as a full matrix. Thus, the advantages stemming from the symmetric and sparse nature of the FEM matrix are not exploited. A modification in the program for this purpose would improve the performance of the implementation of the hybrid method. Further research could be directed towards the extension of the FEM/BEM hybrid method to multigroup problems involving more than two energy groups. A general multiregion formulation with an option for using FEM or BEM for each region could be a topic of further research.

References

Brebbia, C.A., 1978. The Boundary Element Method for Engineers. Pentech Press, London.

Brebbia, C.A., Georgios, P., 1979. Combination of boundary and finite elements in elastostatics. Appl. Math. Models 3 (2), 212–220.

Brebbia, C.A., Telles, J.C.F., Wrobel, L.C., 1984. Boundary Element Techniques. Springer-Verlag, Berlin.

Chiba, G., Tsuji, M., Shimazo, Y., 2001a. A hierarchical domain decomposition boundary element method with a higher order polynomial expansion for solving 2-D multiregion neutron diffusion equations. Ann. Nucl. Energy 28 (9), 895–912.

Chiba, G., Tsuji, M., Shimazo, Y., 2001b. Development of the hierarchical domain decomposition boundary element method for solving the three-dimensionnal multiregion neutron diffusion equations. J. Nucl. Sci. Technol. 38 (8), 664–773.

Courant, R., 1943. Variational methods for the solution of problems of equilibrium and vibrations. Bull. Amer. Math. Soc. 49, 1–23.

Cruse, T.A., Rizzo, F.J., 1968. A direct formulation and numerical solution of the general transient electro-dynamic problem. J. Math. Anal. Appl. 22, 244–259.

Gail, L., Fisher, M., Nackenhorst, U., 2002. FE/BE analysis of structural dynamics and sound radiation from rolling wheels. CMES-Comp. Model. Eng. 3 (6), 815–823.

Guven, I., Madenci, E., 2003. Thermoelastic stress field in a piecewise homogeneous domain under non-uniform temperature using a coupled boundary and finite element method. Int. J. Numer. Meth. Eng. 56 (3), 381–403.

Itagaki, M., 1985. Boundary element methods applied to two-dimensional neutron diffusion problems. J. Nucl. Sci. Technol. 22 (6), 565–583.

Lewis, E.E., 1981. Finite element approximations to the even-parity transport equation. Adv. Nucl. Sci. Technol. 13, 155.

Maiani, M., Montagnini, B., 1999. A boundary element-response matrix method for the multigroup neutron diffusion equations. Ann. Nucl. Energy 26 (15), 1341–1369.

Mikhlin, S.G., 1965. Approximate Solutions of Differential and Integral Equations. Pergamon Press, Oxford.

Ozgener, B., 1990. A comparison of the lumped and consistent source treatments in 3-D finite element calculations. Ann. Nucl. Energy 17 (8), 427–433.

Ozgener, B., 1998. A boundary integral equation for boundary element applications in multigroup neutron diffusion theory. Ann. Nucl. Energy 25 (6), 347–357.

Ozgener, B., Kabadayı, Y., 1996. The acceleration of the finite element solutions of the diffusion theory criticality eigenvalue problems by Chebyshev polynomial extrapolation (in Turkish). In: Proceedings of the Seventh National Meeting on Nuclear Sciences and Technology, Turkey.

Ozgener, B., Ozgener, H.A., 1993. The solution of the criticality eigenvalue problems in the application of the boundary element method to the neutron diffusion equation. Ann. Nucl. Energy 20 (7), 503–518.

Ozgener, B., Ozgener, H.A., 1994. The application of the multiple reciprocity method to the boundary element formulation of the neutron diffusion equation. Ann. Nucl. Energy 21 (11), 711–723.

Ozgener, H.A., Ozgener, B., 2001. A multiregion boundary element method for multigroup neutron diffusion calculations. Ann. Nucl. Energy 28 (6), 585–616.

Pascal, R., Concraux, P., Bergheas, J.M., 2003. Coupling between finite elements and boundary elements for the numerical simulation of introduction heating process using a harmonic balance method. IEEE Trans. Magn. 39 (3), 1535–1538.

Purwadi, M.D., Tsuji, M., Narita, M., Itagaki, M., 1998. The application of the domain decomposition method into the boundary element method for solving the multi-region neutron diffusion equation. Eng. Anal. Boundary Elements 20 (3), 197–204.

Turner, M.J., Clough, R.W., Martin, H.C., Iopp, L.J., 1956. Stiffness and deflation analysis of complex structures. J. Aeronauts Sci. 23 (9), 805–824.

Zienkiewicz, O.C., Kelly, D.W., Buttes, P., 1977. The coupling of finite element method and boundary solution procedures. Int. J. Numer. Meth. Eng. 11, 335–375.